This is a preproof accepted article for *Mineralogical Magazine*

This version may be subject to change during the production process

DOI: 10.1180/mgm.2026.10223

Revision 1

Fe-Ni ordering in meteoritic nickelphosphide, Ni_2FeP

Sergey N. Britvin[1,2]*, Maria G. Krzhizhanovskaya[1], Oleg S. Vereshchagin[1], Natalia S. Vlasenko[1], Arina S. Dorovskaia[1], Renato Pagano[3]†

[1]Saint Petersburg State University, Universitetskaya Nab. 7/9, 199034 St. Petersburg, Russia

[2]Kola Science Center of Russian Academy of Sciences, Fersman Str. 14, 184209 Apatity, Russia

[3]Casella Postale 37, Cinisello (Milano), Italy †

*E-mail: sergei.britvin@spbu.ru

† Deceased

Running title: meteoritic nickelphosphide, Ni_2FeP

Abstract

Nickelphosphide, a Ni-dominant member of the join Ni_3P–Fe_3P, is the second most abundant phosphide in nature, after its Fe-counterpart, schreibersite Fe_3P. Surprisingly, the Fe-Ni distribution in the crystal structure of natural nickelphosphide has never been studied. In this paper, we present the results of X-ray single-crystal study of 13 nickelphosphide samples from different meteorite groups: irons, pallasites (both the main group and the Eagle Station), mesosiderites, and the recently established achondrite grouplet, tissemouminites. The Ni content varies from 1.52 *apfu* (atoms per formula unit), or 50.6 mol.% Ni_3P, in the mineral from the tissemouminite Northwest Africa 1054 (NWA 1054), to 1.87 *apfu* ≡ 62.3 mol.% Ni_3P in phosphide from the Hainholz mesosiderite. The Fe/Ni distribution over the *M*1, *M*2, and *M*3 sites of the crystal structure exhibits a sharp Fe-Ni ordering, with Ni always predominating at the *M*3 and *M*2, leaving the *M*1 site Fe-dominant even in the Ni-richest varieties. This ordering implies that the ideal end-member formula of meteoritic nickelphosphide is Ni_2FeP, rather than the currently adopted Ni_3P. Consequently, the minerals of the considered series can be represented by three different species, with the end members Fe_3P, Ni_2FeP and Ni_3P.

Keywords: schreibersite, nickelphosphide, Fe_3P, Ni_3P, phosphide, meteorite, pallasite, mesosiderite, Ni-rich ataxite, crystal structure

Prepublished article

https://doi.org/10.1180/mgm.2026.10223 Published online by Cambridge University Press

Introduction

The triangle Fe–Ni–P, a chemical backbone of metal-rich planetary interiors, is in the focus of cosmochemical and mineralogical research since the implementation of electron microprobe (EMPA) into geosciences (Goldstein and Ogilvie 1963, 1965; Wood 1964; Reed 1965). Elucidating the origin and thermal history of metal-rich celestial bodies is based on the studies of this system (Goldstein and Short, 1967; Clarke and Goldstein, 1978; Rasmussen et al., 1984; Narayan and Goldstein, 1985; Herpfer *et al.*, 1994). The subjects are, almost exclusively, iron and stony-iron meteorites, whose assemblages serve as natural snapshots of relationships between Fe-Ni metal and phosphides (Romig and Goldstein, 1980, 1981; Reuter *et al.*, 1988; Yang *et al.*, 1996; Goldstein *et al.*, 2009). EMPA was for a long time a sole tool for the study of the join Ni_3P–Fe_3P, until Doenitz (1970) has demonstrated that three independent metal sites in the crystal structure of schreibersite have different affinities towards Fe and Ni; this was a beginning of the implication of X-ray diffraction methods to this system. Since the X-ray based refinement of Fe/Ni ordering is associated with obstacles due to the proximity of their atomic scattering factors, subsequent studies in this field were focused on resonant X-ray diffraction at synchrotron facilities (Moretzki *et al.*, 2003, 2005). However, the recent progress in the X-ray instrumentation allows precise refinement of Fe/Ni site population by means of conventional in-house diffractometers (Britvin *et al.*, 2021ab; Vereshchagin *et al.*, 2026). In this respect it is surprising that Fe-Ni ordering in the crystal structure of natural nickelphosphide, a Ni-dominant member of the join has never been studied by X-ray diffraction methods. Earlier structural studies of this mineral were carried out on synthetic analogues (Rundqvist et al., 1962; Skála and Drabek, 1999, 2000, 2003; Chornkrathok *et al.*, 2020), whereas the refinements of natural terrestrial nickelphosphide did not involve the refinement of Fe/Ni site populations (Galuskin *et al.*, 2025). Meanwhile, it was shown that the Fe/Ni population behavior in natural schreibersite substantially deviates

Prepublished article

https://doi.org/10.1180/mgm.2026.10223 Published online by Cambridge University Press

from that of its synthetic analogue (Britvin *et al.*, 2021a). In this paper we report the first results of an X-ray structural study of natural meteoritic nickelphosphide, which may lead to a possible new look at its chemical formula.

Natural solid solutions Fe_3P–Ni_3P, or schreibersite–nickelphosphide

Schreibersite, $(Fe,Ni)_3P$, is the first phosphide discovered in nature (Berzelius, 1832). Its Ni-dominant counterpart, nickelphosphide, $(Ni,Fe)_3P$, was recognized as distinct mineral relatively recently (Britvin *et al.*, 1999). These phosphides constitute a continuous series of solid solutions Fe_3P–Ni_3P within the metal-rich section of the system Fe–Ni–P (Skála and Drabek, 1999, 2000, 2003; Britvin *et al.*, 2021a). Despite the obvious chemical distinction between Fe- and Ni-dominant members, they are often labeled by the common name "schreibersite" (e.g., Skála and Drábek, 1999, 2000; Skála and Císařová, 2005; Chornkrathok et al., 2020), which in such cases should be treated as a series name, similar to, e.g., olivine or plagioclase series. The relationships within the system Fe–Ni–P are quite complex, including more than a dozen of different phosphides (Doan and Goldstein 1970; Drabek, 2006; Schmetterer *et al.*, 2009; Britvin *et al.*, 2020c), the majority of which have been discovered in nature for the last two decades (Buseck, 1969; Britvin *et al.*, 2002, 2019ab, 2021abc; 2022; Pratesi *et al.*, 2006). However, it is the join Fe_3P–Ni_3P that represents a backbone of cosmochemistry of reduced phosphorus, being an integral part of the metal-phosphide system (Goldstein and Ogilvie 1963, 1965; Reed 1965; Buchwald, 1966, 1975, 1977; Chornkrathok et al., 2020). Shreibersite is a common accessory phase of lunar regolith (Pasek, 2015). It is suggested that schreibersite was the very primary phosphorus-bearing phase crystallized during the condensation of protoplanetary nebula (Pasek, 2019).

Pure or nearly pure schreibersite, Fe_3P, of various geneses, has been reported from several terrestrial localities. The mineral of magmatic origin is known in basalts of Disko Island, Greenland (Pauly, 1969; Pedersen, 1981; Vereshchagin *et al.*, 2024a). It is confined to

Preprint article

https://doi.org/10.1180/mgm.2026.10223 Published online by Cambridge University Press

native iron assemblages formed by partial reduction of lithophile iron on contact with coal-bearing sediments. Schreibersite is a characteristic, though uncommon mineral in coal deposits, where it is a semi-anthropogenic product in reduced assemblages of burnt coal dumps, e.g., in Commentry and Cranzac, France (Palache *et al.*, 1944); Urals, Russia (Nishanbaev et al., 2002); and Silesia, Poland (Ciesielczuk *et al.*, 2015). One of the most enigmatic finds of schreibersite was its pseudomorph after wood collected by the Pisces-class submersible in the Read Sea rift zone, on the seafloor at a depth of 1400 m (Borodaev *et al.*, 1982). Findings of terrestrial schreibersite in fulgurites, the products of lightning-induced fusion of sedimentary rocks, suggest that fulgurites could be a possible source of reactive prebiotic phosphorus on early Earth (e.g., Pasek and Lauretta, 2005; Pasek *et al.*, 2007; Pasek, 2008, 2017; Pasek and Block, 2009; Pasek *et al.*, 2013, 2017; Plyashkevich *et al.*, 2016). Another scenario for the formation of terrestrial schreibersite is realized in pyrometamorphic complexes of Middle East and Mongolia, where phosphide assemblages were formed during combustion metamorphism of carboniferous sediments (Britvin *et al.*, 2015; 2017b; 2021a; Savina *et al.*, 2020; Murashko *et al.*, 2022; Galuskin *et al.* 2024, 2025; Vereshchagin *et al.*, 2024b). Schreibersite of likely meteoritic origin was identified in Agoudal impact site, Morocco (Schmieder *et al.*, 2015).

Meteoritic shreibersite always contains substantial percentage of Ni substituting for Fe (Britvin *et al.*, 2021a). Nickelphosphide, until the recent findings in the Middle East and Greenland (Galuskin *et al.* 2024, 2025; Vereshchagin *et al.*, 2024a), was known only in meteorites (Britvin *et al.*, 1999), where the most nickeliferous mineral from the Oktibbeha County ataxite contains 76 mole % of Ni_3P (Reed, 1972). Both schreibersite and nickelphosphide are ubiquitous in almost all iron meteorites (Goldstein and Ogilvie 1963, 1965; Reed 1965; Buchwald, 1966, 1975, 1977; Britvin et al., 1999, 2021a); schreibersite may constitute more than 20 vol.% of the metal phase (Kotomaa *et al.*, 2025). Schreibersite

Preprinted article

https://doi.org/10.1180/mgm.2026.10223 Published online by Cambridge University Press

from iron meteorites has been thoroughly studied (see the references cited above). In striking contrast, the stony-irons are, in fact, virtually unexplored in this regard. The published papers dedicated to stony-irons point the accent on silicate, phosphate, chromite, or rarely, Fe-Ni metal chemistry, almost completely ignoring the chemistry of phosphides (e.g., Powell, 1969, 1971; Buseck, 1977; Buseck and Holdsworth, 1977; Scott, 1977; Mittlefehldt *et al.*, 1979; Rubin and Mittlefehldt, 1992; Patzer *et al.*, 2004; Lucas *et al.*, 2019; García *et al.*, 2022; Mittlefehldt, 2024). There are two rare phosphide minerals discovered in pallasites - barringerite, Fe_2P, and nazarovite, $Ni_{12}P_5$ (Buseck, 1969; Britvin *et al.*, 2022a), and one more in the meteorite of the tissemouminite group - melliniite, $(Ni,Fe)_4P$ (Pratesi *et al.*, 2006). Surprisingly, there are no even approaches to classify the compositional data on the minerals of schreibersite-nickelphosphide series in stony-irons. The scarce records are limited to brief mentions of "phosphide" or "schreibersite" with, at most, approximate estimations of Ni content (Kulpecz and Hewins, 1978; Agosto *et al.*, 1980). The present study, being focused on nickelphosphide, partially completes this gap.

Samples and analytical methods

Meteorite samples

The inventory used in this research included 13 samples from 3 mesosiderites, 2 tissemouminites, 2 main-group pallasites, the Eagle Station pallasite, and 3 iron meteorites (Table 1). The selection of meteorites was based on two criteria: the availability of the samples for study, both in general and for destructive analytical methods (i.e., X-ray structural analysis), and the mandatory presence of nickelphosphide, $(Ni,Fe)_3P$ with Ni>Fe. Mesosiderites are comprised by Budulan and Mincy, both representatives of the B4 subgroup, and Hainholz, a member of the A4 subgroup. The details of their petrology, mineralogy and geochemistry can be found in previous works (e.g., Powell 1969, 1971; Mittlefehldt *et al.*, 1979; Nehru *et al.*, 1980; Hewins, 1984; Mittlefehldt, 1990; Rubin and Mittlefehldt, 1992;

Prepublished article

https://doi.org/10.1180/mgm.2026.10223 Published online by Cambridge University Press

Albrecht *et al.*, 2000; Quitté *et al*. 2005; Lorenz *et al*., 2010; Haba *et al*., 2019; García *et al*., 2022; Iannini Lelarge *et al*., 2022; Sugiura *et al.*, 2022; Kouvatsis *et al*., 2023). Northwest Africa 725 (NWA 725) and NWA 1054, originally classified as acapulcoites or winonaites (Patzer *et al*., 2004; Pratesi *et al*., 2006; Greenwood *et al*. 2012; Hidaka *et al*., 2019; Lucas *et al*., 2019; Zeng *et al.*, 2019), were recently proposed to reconsider into a separate transient group – tissemouminites (Stephant *et al*., 2022). Pallasites are comprised by Brahin and Finmarken, both the members of pallasite main group (for their petrology and geochemistry see, e.g., Yang *et al.*, 2010; Boesenberg *et al.*, 2012; McKibbin *et al.*, 2013, 2019; Mittlefehldt, 2024), and the Eagle Station, a prototype member of the eponymous group (Scott, 1977; Teplyakova *et al*., 2022; Mittlefehldt, 2024). Three Ni-rich iron meteorites were included because they contain compositionally equilibrated nickelphosphide, $(Ni,Fe)_3P$, different from Fe-Ni zoned "rhabdite" (Reed, 1965; Buchwald, 1975, 1977; Clarke and Goldstein, 1978) common to most of iron meteorites. Butler (iron ungrouped) and Dorofeevka (IIF) are plessitic octahedrites containing ~15 wt.% Ni (Goldstein, 1966; Buchwald, 1975; Kracher *et al*., 1980; Hilton *et al*., 2020). Butler is a type meteorite for nickelphosphide (Britvin *et al.*, 1999). The meteorite is known for extreme enrichment in Ge (2000 μg/g, or 0.2 wt.% in bulk metal); it is a structural and compositional analogue of NWA 859, or the Taza iron (Wasson, 2011). Barbianello (iron ungrouped), containing 27 wt.% Ni, belongs to a small group of nickel-rich ataxites enriched in phosphides and carbides (Fioretti and Zipfel, 2004; Britvin *et al.*, 2019; Vereshchagin *et al.*, 2026).

Electron microprobe analysis (EMPA)

The samples, comprised by the pieces up to 1 cm in the maximum dimension, were embedded into epoxy pellets, which were ground and polished by conventional methods. The study included microscopic investigation of polished sections in reflected light, followed by EMPA of selected areas. The latter was carried out on carbon-coated sections in the

Prepublished article

https://doi.org/10.1180/mgm.2026.10223 Published online by Cambridge University Press

Geomodel Resource Center of Saint-Petersburg State University, by means of an INCA WAVE 500 WDX spectrometer (20 kV, 15 nA) attached to a Hitachi S-3400N scanning electron microscope, using *K*α-lines and pure Ni, Fe, Co metals and InP as analytical standards.

Single-crystal X-ray diffraction (SCXRD) and powder X-ray diffraction (PXRD)

X-ray studies were carried out on the EMPA-analyzed single-crystal grains manually extracted from the analyzed polished sections with a tungsten carbide needle. Owing to the brittleness of nickelphosphide, mechanical extraction does not lead to its structural destruction. For SCXRD data collection, three diffractometer models were available: Bruker APEX II (CCD detector), Bruker Kappa APEX DUO (CCD detector) and Rigaku-Oxford Diffraction XtaLAB Synergy-S (HPC detector), all being equipped with sealed X-ray tubes (Mo*K*α-radiation). For each crystal intended for the study, the choice of suitable instrument was made based on the crystal size/collection time criteria. The ground requirements were the same as in the recent study of schreibersite (Britvin *et al.*, 2021a): full Ewald sphere up to at least 2θ = 64°, frame width 1°, average $I > 30\sigma(I)$. After completion of SCXRD data collection and proof of their quality using preliminary crystal structure refinements, the broken-off fragments of studied crystals were powdered for the obtaining of PXRD data. The latter were collected by means of a Rigaku RAXIS Rapid II diffractometer equipped with a semi-cylindrical imaging plate (r = 128.4 mm), rotating anode (Co*K*α-radiation, 40 kV, 15 mA) and mirror microfocus monochromator. Exposure time for each sample was set between 30 and 60 min, depending on the sample size. In case of very small (less than 15 μm) crystal fragments of nickelphosphide from Barbianello and Dorofeevka, the PXRD data were obtained on single crystals with implementation of a Gandolfi method. The 2D PXRD images were transformed into the XY profiles with osc2xrd program (Britvin *et al.*, 2017), and the resultant profiles were used for precise unit-cell parameter determination by a full-profile

Prepublished article

https://doi.org/10.1180/mgm.2026.10223 Published online by Cambridge University Press

Rietveld refinement (Bruker TOPAS v.5.0 software). Fe/Ni input occupancy factors were taken from single-crystal structure refinements and were not refined. The final single-crystal structure refinements, using the refined PXRD unit-cell parameters, were carried out by means of *SHELX*-2018 set of programs (Sheldrick, 2015) incorporated into the Olex2 v. 1.5 graphical user shell (Dolomanov *et al.*, 2009). The Fe/Ni occupancy factors were refined for each metal site. In case when site occupancy factor for either Fe or Ni was equal to unity within the 2σ tolerance, the site was assumed to be fully occupied by the corresponding element. The summary of data collection and structure refinement details is presented in Table 2; the full details can be retrieved from Crystallografic Informatiom Files (CIF) included into the Supplementary material.

Results

Occurrence of nickelphosphide

Iron meteorites and pallasites

The common appearance of nickelphosphide in studied irons and pallasites is presented in Figure 1. The occurrence and assemblages follow the trends known for the same meteorites and their structural analogues (e.g., Buchwald, 1966, 1975, 1977; Buseck 1977; Buseck and Holdsworth, 1977). In plessitic octahedrites Butler and Dorofeevka, the mineral occurs as isolated, round to angular single-crystal grains from 10 to 200 μm in size confined to α-(Fe,Ni) (kamacite) fields and veinlets within plessite - a microgranular variety of Widmanstätten structure (Fig. 1a). In Barbianello, a nickel-rich ataxite, the euhedral to long-prismatic crystals of nickelphosphide grow on the walls of the kamacite-filled micro-pockets within the taenite matrix (Fig. 1b, see also Vereshchagin *et al.*, 2026). In the Brahin, Eagle Station and Finmarken pallasites, the mineral occurs as crystalline encrustations and rims several hundred micrometers in largest dimension, tracking the kamacite-plessite interfaces; its aggregates can reach several hundred micrometers in largest dimension (Fig. 1c).

Preprinted article

https://doi.org/10.1180/mgm.2026.10223 Published online by Cambridge University Press

Mesosiderites and tissemouminites

The appearance and assemblages of nickelphosphide in these meteorites is shown in Fig. 2. In mesosiderites (Budulan, Mincy and Hainholz), the mineral forms very sharp, well developed isometric crystals confined to submillimeter- to millimeter-sized kamacite fields (Fig. 2ab). The crystals, always sitting on the rock-forming clinopyroxene crystals, are ingrown into the kamacite-filled pockets. This type of occurrence is the same as it was described in the Emery mesosiderite (Kulpecz and Hewins, 1978).

In tissemouminites NWA 725 and NWA 1054, nickelphosphide associations are more diverse than in mesosiderites. In addition to common kamacite assemblages, one can observe nickelphosphide crystals penetrating tetrataenite–rimmed plessite fields (Fig. 2c). Troilite is quite common in these assemblages, alongside with rare native copper patches (Fig. 2d). The relationships with rock-forming silicates could not be traced, because both examined tissemoumintes have underwent severe terrestrial weathering, and direct contacts of nickelphosphide with silicates were not encountered. It is noteworthy that NWA 1054 is known as a type occurrence for another phosphide, melliniite $(Ni,Fe)_4P$ (Pratesi *et al.*, 2006). In this regard, it should be noted that out of the more than 200 phosphide grains studied in several sections of this meteorite, melliniite was not observed.

Chemical composition

The composition of studied nickelphosphide grains is summarized in Table 1. The Ni contents vary between 44.1 and 53.7 wt. % that corresponds to 1.52 - 1.87 Ni atoms per M_3P formula unit (Table 3). All inspected grains are chemically homogeneous, with no signs of Fe/Ni zoning, a feature of rhabdite (the late acicular variety of schreibersite-nickelphosphide typical of coarse- to medium-structured octahedrites) (Cohen, 1894; Goldstein and Ogilvie, 1963; Reed, 1965; Clarke and Goldstein, 1978).

Prepublished article

https://doi.org/10.1180/mgm.2026.10223 Published online by Cambridge University Press

Fe-Ni ordering in the crystal structure of nickelphosphide

Nickelphosphide crystallizes in tetragonal system, in a non-centrosymmetric space group $I\bar{4}$ (# 82). The crystal structure of its Fe-dominant counterpart, schreibersite, was studied in detail by many authors (e.g., Britvin et al., 2021a and references cited therein). It contains one phosphorus site coordinated by 9 both metal and P atoms, and three metal sites, which are denoted as *M*1 (CN = 15), *M*2 (CN = 14) and *M*3 (CN = 13) according to Doenitz (1970). The structure of synthetic analogues of Fe-bearing nickelphosphide was studied by Skála and Drabek (1999, 2000, 2003). However, the data on natural mineral were never reported before. The refined Ni occupancies for the *M*1, *M*2 and *M*3 sites of the crystal structure of meteoritic nickelphosphide are given in Table 3. The most interesting observation that becomes obvious from this table is that Ni almost completely avoids the incorporation into the *M*1 site throughout the compositional range, from the relatively Ni-poor boundary mineral of NWA 1054 to the most Ni-rich member from Hainholz. This tendency was known in schreibersite (Doenitz, 1970 and the referring works). However, in nickelphosphide, where Ni overrides Fe in the total atomic percentage, it leads to the emergence of site-ordered phosphide phase whose general structural formula can be represented as $^{M1}Fe^{M2}(Ni,Fe)^{M3}NiP$ or ideally Ni_2FeP.

Discussion and conclusion

The existence of an ordered meteoritic phosphide with the ideal composition Ni_2FeP raises the question of the chemical formula of nickelphosphide, the second most abundant phosphide in meteoritic matter. This mineral was first described from the Butler meteorite as the Ni-dominant member of the supposed continuous series of solid solutions Ni_3P–Fe_3P (Britvin et al., 1999). The structural study of natural nickelphosphide, in particular revelation of the Fe-Ni ordering, was impossible at that time, therefore its ideal formula was assumed to be Ni_3P (Britvin et al., 1999). Subsequently, a series of structural studies were carried out

Preprinted article

https://doi.org/10.1180/mgm.2026.10223 Published online by Cambridge University Press

using single-crystal X-ray diffraction and the Rietveld method (Skála and Drabek, 1999, 2000, 2003), but precise determinations of Fe/Ni ordering were not reported. In our study, there is clear evidence that meteoritic nickelphosphide has the ideal formula Ni_2FeP rather than Ni_3P. It is important to note that this formula is also valid for the mineral from the Butler meteorite (Table 3), the type occurrence of original nickelphosphide (Britvin et al., 1999). The next substantial consequence of our study is that the existence of meteoritic phosphide with an ideal formula approaching Ni_3P seems unlikely. Provided that the specific affinity of Ni towards *M*3 and *M*2 sites is a universal feature of the schreibersite-nickelphosphide structure, the predominance of Ni at the Ni-poor *M*1 site could only be achieved in a mineral containing more than 2.50 Ni per formula unit, or 83 mol.% Ni_3P. This threshold has never been reached in meteoritic nickelphosphide, and the geochemical or structural reasons of such behavior require further investigations. However, some Ni-richest varieties of terrestrial nickelphosphide from the Hatrurim Formation, Jordan (Galuskin *et al.*, 2024, 2025) might satisfy the requirements of all-site Ni predomination, approaching the Ni_3P end-member. Consequently, the minerals of the considered series can be comprised by different species, the end members of wich are Fe_3P, Ni_2FeP and Ni_3P.

Supplementary material. The supplementary material for this article can be found at https://doi.org/10.1180/mgm***

Acknowledgements. The authors are grateful to the referees for valuable reviews and suggestions, as well as to the Editor, Stuart Mills, for editorial handling of the manuscript. The authors thank the Resource Center of X-ray diffraction studies and Geomodel Resource Centre of Saint-Petersburg State University for providing instrumental and computational resources.

Financial statement. This study was carried out with the financial support of Russian Science Foundation, grant 23-77-10025.

Preprinted article

https://doi.org/10.1180/mgm.2026.10223 Published online by Cambridge University Press

Competing interests. The authors declare none.

References

Agosto W.N., Hewins R.H. and Clarke R.S., Jr. (1980) Allan Hills A77219, the first Antarctic mesosiderite. *Proceedings of Lunar Planetary Conference*, **11**, 1027–1045.

Albrecht A., Schnabel C., Vogt S., Xue S., Herzog G.F., Begemann F., Weber H.W., Middleton R., Fink D. and Klein J. (2000) Light noble gases and cosmogenic radionuclides in Estherville, Budulan, and other mesosiderites: implications for exposure histories and production rates. *Meteoritics & Planetary Science*, **35**, 975–986, https://doi.org/10.1111/j.1945-5100.2000.tb01486.x

Berzelius J.J. (1832) Undersökning af en vid Bohumiliz I Böhmen funnen jernmassa. *Kongelige Svenska Vetenskaps-Academiens Handlingar*, 106–119.

Boesenberg J.S., Delaney J.S. and Hewins R.H. (2012) A petrological and chemical reexamination of Main Group pallasite formation. *Geochimica et Cosmochimica Acta*, **89**, 134–158, https://doi.org/10.1016/j.gca.2012.04.037

Borodaev Y.S., Bogdanov Y.A. and Vyalsov L.N. (1982) New nickel-free variety of schreibersite Fe_3P. *Zapiski Vsesoyuznogo Mineralogicheskogo Obschestva*, **111**, 682–687 (in Russian).

Britvin S.N., Kolomensky V.D., Boldyreva M.M., Bogdanova A.N., Kretser Yu.L., Boldyreva O.N. and Rudashevsky N.S. (1999) Nickelphosphide $(Ni,Fe)_3P$ – the nickel analog of schreibersite. *Proceedings of the Russian Mineralogical Society*, **128**, 64–72 (in Russian).

Britvin S.N., Rudashevsky N.S., Krivovichev S.V., Burns P.C. and Polekhovsky Y.S. (2002) Allabogdanite, $(Fe,Ni)_2P$, a new mineral from the Onello meteorite: The occurrence and crystal structure. *American Mineralogist*, **87**, 1245–1249, https://doi.org/10.2138/am-2002-8-924

Britvin S.N., Murasko M.N., Vapnik Y., Polekhovsky Y.S. and Krivovichev S.V. (2015) Earth's phosphides in Levant and insights into the source of Archaean prebiotc phosphorus. *Scientific Reports*, **5**, 8355, https://doi.org/10.1038/srep08355

Britvin S.N., Dolivo-Dobrovolsky D.V. and Krzhizhanovskaya M.G. (2017a) Software for processing of X-ray powder diffraction data obtained from the curved image plate detector of Rigaku RAXIS Rapid II diffractometer. *Proceedings of the Russian Mineralogical Society*, **146(3)**, 104–107 (in Russian).

Britvin S.N., Murashko M.N., Vapnik E., Polekhovsky Y.S. and Krivovichev S.V. (2017b) Barringerite Fe_2P from pyrometamorphic rocks of the Hatrurim Formation, Israel. *Geology of Ore Deposits*, **59**, 619–625, https://doi.org/10.1134/S1075701517070029

Britvin S.N., Murashko M.N., Vapnik Ye., Polekhovsky Yu.S., Krivovichev S.V., Vereshchagin O.S. Vlasenko N.S. Shilovskikh V.V. and Zaitsev A.N. (2019a) Zuktamrurite, FeP_2, a new mineral, the phosphide analogue of löllingite, $FeAs_2$. *Physics and Chemistry of Minerals*, **46**, 361–369, https://doi.org/10.1007/s00269-018-1008-4

Britvin S.N., Vapnik Ye., Polekhovsky Yu.S., Krivovichev S.V., Krzhizhanovkaya M.G., Gorelova L.A., Vereshchagin O.S., Shilovskikh V.V. and Zaitsev A.N. (2019b) Murashkoite, FeP, a new terrestrial phosphide from pyrometamorphic rocks of the Hatrurim Formation,

Preprinted article

https://doi.org/10.1180/mgm.2026.10223 Published online by Cambridge University Press

Southern Levant. *Mineralogy and Petrology*, **113**, 237–248, https://doi.org/10.1007/s00710-018-0647-y

Britvin S.N., Shilovskikh V.V., Pagano R., Vlasenko N.S., Zaitsev A.N., Krzhizhanovskaya M.G., Lozhkin M.S., Zolotarev A.A. and Gurzhiy V.V. (2019c) Allabogdanite, the high-pressure polymorph of $(Fe,Ni)_2P$, a stishovite-grade indicator of impact processes in the Fe–Ni–P system. *Scientific Reports*, **9**, 1047, https://doi.org/10.1038/s41598-018-37795-x

Britvin S.N., Murashko M.N., Vapnik Y., Polekhovsky Y.S., Krivovichev S.V., Krzhizhanovskaya M.G., Vereshchagin O.S., Shilovskikh V.V. and Vlasenko N.S. (2020a) Transjordanite, Ni_2P, a new terrestrial and meteoritic phosphide, and natural solid solutions barringerite–transjordanite (hexagonal Fe_2P-Ni_2P). *American Mineralogist*, **105**, 428–436, https://doi.org/10.2138/am-2020-7275

Britvin S.N., Murashko M.N., Vapnik Y., Polekhovsky Y.S., Krivovichev S.V., Vereshchagin O.S., Shilovskikh V.V., Vlasenko N.S. and Krzhizhanovskaya M.G. (2020b) Halamishite, Ni_5P_4, a new terrestrial phosphide in the Ni-P system. *Physics and Chemistry of Minerals*, **47**, 3–7, https://doi.org/10.1007/s00269-019-01073-7

Britvin S.N., Murashko M.N., Vapnik Y., Polekhovsky Y.S., Krivovichev S.V., Vereshchagin O.S., Shilovskikh V.V. and Krzhizhanovskaya M.G. (2020c) Negevite, the pyrite-type NiP_2, a new terrestrial phosphide. *American Mineralogist*, **105**, 422–427, https://doi.org/10.2138/am-2020-7192

Britvin S.N., Krzhizhanovskaya M.G., Zolotarev A.A., Gorelova L.A., Obolonskaya E.V., Vlasenko N.S., Shilovskikh V.V. and Murashko M.N. (2021a) Crystal chemistry of schreibersite, $(Fe,Ni)_3P$. *American Mineralogist*, **106**, 1520–1529, https://doi.org/10.2138/am-2021-7766

Britvin S.N., Krivovichev S.V., Vereshchagin O.S., Vlasenko N.S., Shilovskikh V.V., Krzhizhanovskaya M.G., Lozhkin M.S., Obolonskaya E.V. and Kopylova Y.O. (2021b) Perryite, $(Ni,Fe)_{16}PSi_5$, from the Mount Egerton aubrite: the first natural P-Si-ordered phosphide-silicide. *Journal of Geosciences*, **66**, 189–198, https://doi.org/10.3190/jgeosci.331

Britvin S.N., Murashko M.N., Krzhizhanovskaya M.G., Vereshchagin O.S., Vapnik Ye., Shilovskikh V.V., Lozhkin M.S. and Obolonskaya E.V. (2022a) Nazarovite, $Ni_{12}P_5$, a new terrestrial and meteoritic mineral structurally related to nickelphosphide, Ni_3P. *American Mineralogist*, **107**, 1946–1951, https://doi.org/10.2138/am-2022-8219

Buchwald V.F. (1966) The Iron-Nickel-Phosphorus System and the Structure of Iron Meteorites. *Acta Polytechnica Scandinavica*, **51**, 45 p.

Buchwald V.F. (1975) Handbook of iron meteorites. University of California Press, Berkeley.

Buchwald V.F. (1977) The mineralogy of iron meteorites. *Philosophical Transactions of the Royal Society*, **A286**, 453–491, https://doi.org/10.1098/rsta.1977.0127

Buseck P.R. (1969) Phosphide from meteorites: barringerite, a new iron-nickel mineral. *Science*, **165**, 169–171, https://doi.org/10.1126/science.165.3889.169

Buseck P.R. (1977) Pallasite meteorites - Mineralogy, petrology and geochemistry. *Geochimica et Cosmochimica Acta*, **41**, 711–740, https://doi.org/10.1016/0016-7037(77)90044-8

Buseck P.R. and Holdsworth E. (1977) Phosphate minerals in pallasite meteorites. *Mineralogical Magazine*, **41**, 91–102, https://doi.org/10.1180/minmag.1977.041.317.14

Pre-published article

https://doi.org/10.1180/mgm.2026.10223 Published online by Cambridge University Press

Chornkrathok S., Zhang D.Z. and Dera P. (2020) Structure and behavior of the Ni end-member schreibersite Ni_3P under Compression to 50 GPa. *Minerals*, **10**, 306, https://doi.org/10.3390/min10040306

Ciesielczuk J., Kruszewski Ł. and Majka J. (2015) Comparative mineralogical study of thermally altered coal-dump waste, natural rocks and the products of laboratory heating experiments. *International Journal of Coal Geology*, **139**, 114–141, https://doi.org/10.1016/j.coal.2014.08.013

Clarke R.S. and Goldstein J.I. (1978) Schreibersite growth and its influence on the metallography of coarse-structured iron meteorites. *Smithsonian Contributions to Earth Sciences*, **21**, 1–80.

Cohen E. (1894) Meteoreisen-Studien III: Rhabdit. *Annalen des K.K. Naturhistorischen Hofmuseums*, **IX**, 97–118.

Doan A.S. and Goldstein J.I. (1970) The ternary phase diagram, Fe-Ni-P. *Metallurgical Transactions*, **1**, 1759–1767, https://doi.org/10.1007/BF02642026

Doenitz F.D. (1970) Die Kristallstructur des meteoritischen Rhabdits $(Fe,Ni)_3P$. *Zeitschrift für Kristallographie*, **A131**, 232–236, https://doi.org/10.1524/zkri.1970.131.16.222

Dolomanov O.V., Bourhis L.J., Gildea R.J., Howard J.A. and Puschmann H. (2009) OLEX2: a complete structure solution, refinement and analysis program. *Journal of Applied Crystallography*, **42**, 339–341, https://doi.org/10.1107/S0021889808042726

Drabek M. (2006) Phosphide solid-solutions within the metal-rich portion of the quarternary system Co-Fe-Ni-P at 800 °C, and mineralogical implications. *Canadian Mineralogist*, **44**, 399–408, https://doi.org/10.2113/gscanmin.44.2.399

Essene E.J. and Fisher D.C. (1986) Lightning strike fusion- extreme reduction and metal-silicate liquid immiscibility. *Science*, 234, 189–193, https://doi.org/10.1126/science.234.4773.1

Fioretti A.M. and Zipfel J. (2004) Barbianello: An ungrouped nickel-rich iron meteorite found in Italy. *Meteoritics & Planetary Science*, **39** (8 Suppl.), A143–A149, https://doi.org/10.1111/j.1945-5100.2004.tb00350.x

Galuskin E.V., Galuskina I.O., Kusz J., Książek M., Vapnik Ye. and Zieliński G. (2024) Karwowskiite, $Ca_9(Fe^{2+}_{0.5}\square_{0.5})Mg(PO_4)_7$ – A New Merrillite Group Mineral from Paralava of the Hatrurim Complex, Daba-Siwaqa, Jordan. *Minerals*, **14**, 825, https://doi.org/10.3390/min14080825

Galuskin E.V., Galuskina I.O., Vapnik Ye., Kusz J., Marciniak-Maliszewska B. and Zieliński G. (2025) Two modes of terrestrial phosphide formation. *American Mineralogist*, **110**, 547–559, https://doi.org/10.2138/am-2024-9315

García L.N., Varela M.E., Hwang S.-L., Shen P., Bolmaro R. and Ávalos M. (2022) Mincy Mesosiderite Metallic Nodules Analyzed by EBSD: An Approach to Understanding their Thermal History. *Meteoritics & Planetary Science*, **57**, 1958–1972, https://doi.org/10.1111/maps.13911

Goldstein J.I. and Ogilvie R.E. (1963) Electron microanalysis of Metallic Meteorites, Part.1: Phosphides and Sulfides. *Geochimica et Cosmochimica Acta*, **27**, 623–637, https://doi.org/10.1016/0016-7037(63)90015-2

Pre-published article

https://doi.org/10.1180/mgm.2026.10223 Published online by Cambridge University Press

Goldstein J.I. and Ogilvie R.E. (1965) The growth of the Widmanstatten pattern in metallic meteorites. *Geochimica et Cosmochimica Acta*, **29**, 893–920, https://doi.org/10.1016/0016-7037(65)90085-2

Goldstein J.I. and Short J.M. (1967) The iron meteorites, their thermal history and parent bodies. *Geochimica et Cosmochimica Acta*, **31**, 1733–1770, https://doi.org/10.1016/0016-7037(67)90120-2

Goldstein J.I., Scott E.R.D. and Chabot N.L. (2009) Iron Meteorites: Crystallization, Thermal History, Parent Bodies, and Origin. *Chemie der Erde*, **69**, 293–325, https://doi.org/10.1016/j.chemer.2009.01.002

Greenwood R.C., Franchi I.A., Gibson J.M. and Benedix G.K. (2012) Oxygen isotope variation in primitive achondrites: the influence of primordial, asteroidal and terrestrial processes. *Geochimica et Cosmochimica Acta*, **94**, 146–163, https://doi.org/10.1016/j.gca.2012.06.025

Haba M.K., Wotzlaw J.-F., Lai Y.-J., Yamaguchi A. and Schönbächler M. (2019) Mesosiderite formation on asteroid 4 Vesta by a hit-and-run collision. *Nature Geoscience*, **12**, 510–515, https://doi.org/10.1038/s41561-019-0377-8

Herpfer M.A., Larimer J.W. and Goldstein J.I. (1994) A comparison of metallographic cooling rate methods used in meteorites. *Geochimica et Cosmochimica Acta*, **58**, 1353–1365, https://doi.org/10.1016/0016-7037(94)90387-5

Hewins R.H. (1984) The case for a melt matrix in plagioclase-POIK mesosiderites. *Journal of Geophysical Research*, **89** (Suppl.), C289–C297, https://doi.org/10.1029/JB089iS01p0C289

Hidaka Y., Shirai N., Yamaguchi A. and Ebihara M. (2019) Siderophile Element Characteristics of Acapulcoite–Lodranites and Winonaites: Implications for the Early Differentiation Processes of their Parent Bodies. *Meteoritics & Planetary Science*, **54**, 1153–1166, https://doi.org/10.1111/maps.13273

Hilton C.D., Ash R.D. and Walker R.J. (2020) Crystallization histories of the group IIF iron meteorites and Eagle Station pallasites. *Meteoritics & Planetary Science*, **55**, 2570–2586, https://doi.org/10.1111/maps.13602

Iannini Lelarge S., Folco L., Masotta M., Greenwood R.C., Russell S.S. and Bates H.C. (2022) Asteroids accretion, differentiation, and break-up in the Vesta source region: Evidence from cosmochemistry of mesosiderites. *Geochimica et Cosmochimica Acta*, **329**, 135–151, https://doi.org/10.1016/j.gca.2022.05.003

Kotomaa L., Väisänen M., Heinonen J.S., Mäkilä E., O'Brien H. and Peltola A. (2025) Löpönvaara: a new phosphorus-rich iron meteorite from Finland. *Meteoritics & Planetary Science*, **60**, 2442–2457, https://doi.org/10.1111/maps.70049

Kouvatsis I., Cartwright J.A. and Whitehouse M.J. (2023) Lead-lead (Pb-Pb) dating of eucrites and mesosiderites: implications for the formation and evolution of Vesta. *Geochimica et Cosmochimica Acta*, **348**, 369–380, https://doi.org/10.1016/j.gca.2023.03.026

Kracher A., Willis J. and Wasson J.T. (1980) Chemical classification of iron meteorites-IX. A new group (IIF), revision of IAB and IIICD, and data on 57 additional irons. *Geochimica et Cosmochimica Acta*, **44**, 773–787, https://doi.org/10.1016/0016-7037(80)90259-8

Preprint published article

https://doi.org/10.1180/mgm.2026.10223 Published online by Cambridge University Press

Kulpecz A.A. Jr. and Hewins R.H. (1978) Cooling rate based on schreibersite growth for the Emery mesosiderite. *Geochimica et Cosmochimica Acta*, **42**, 1495–1500, https://doi.org/10.1016/0016-7037(78)90020-0

Lorenz C.A., Nazarov M.A., Brandstaetter F. and Ntaflos T. (2010) Metasomatic Alterations of Olivine Inclusions in the Budulan Mesosiderite. *Petrology*, **18**, 461–470, https://doi.org/10.1134/S0869591110050012

Lucas M.P., Emery J.P., Hiroi T. and McSween H.Y. (2019) Spectral properties and mineral compositions of acapulcoite–lodranite clan meteorites: establishing S-type asteroid–meteorite connections. *Meteoritics & Planetary Science*, **54**, 157–180, https://doi.org/10.1111/maps.13203

McKibbin S.J., O'Neill H.S.C., Mallmann G. and Halfpenny A. (2013) LA-ICP-MS mapping of olivine from the Brahin and Brenham meteorites: complex elemental distributions in the pallasite olivine precursor. *Geochimica et Cosmochimica Acta*, **119**, 1–17, https://doi.org/10.1016/j.gca.2013.05.031

McKibbin S.J., Pittarello L., Makarona C., Hamann C., Hecht L., Chernonozhkin S.M., Goderis S. and Claeys P. (2019) Petrogenesis of main group pallasite meteorites based on relationships among texture, mineralogy, and geochemistry. *Meteoritics & Planetary Science*, **54**, 2814–2844, https://doi.org/10.1111/maps.13392

Mittlefehldt D.W. (1990) Petrogenesis of Mesosiderites: I. Origin of Mafic Lithologies and Comparison with Basaltic Achondrites. *Geochimica et Cosmochimica Acta*, **54**, 1165–1173, https://doi.org/10.1016/0016-7037(90)90447-S

Mittlefehldt D.W. (2024) Geochemistry of pallasite olivine and the origin of pallasites. *Geochimica et Cosmochimica Acta*, **383**, 92–107, https://doi.org/10.1016/j.gca.2024.08.010

Mittlefehldt D.W., Chou C.-L. and Wasson J.T. (1979) Mesosiderites and howardites: igneous formation and possible genetic relationships. *Geochimica et Cosmochimica Acta*, **43**, 673–688, https://doi.org/10.1016/0016-7037(79)90252-7

Moretzki O., Doering Th., Geist V., Morgenroth W. and Wendschuh M. (2003) Crystal structure of iron nickel phosphide, $Fe_{1.8}Ni_{1.2}P$, a Schreibersite extracted from Orange River meteorite. *Zeitschrift für Kristallographie - New Crystal Structures*, **218**, 395–396, https://doi.org/10.1524/ncrs.2003.218.4.395

Moretzki O., Morgenroth W., Skála R., Scymanski A., Wendschuh M. and Geist V. (2005) Determination of metal ordering in meteoritic $(Fe,Ni)_3P$ crystals. *Journal of Synchrotron Radiation*, **12**, 234–240, https://doi.org/10.1107/S0909049504028237

Murashko M.N., Britvin S.N., Vapnik Y., Polekhovsky Y.S., Shilovskikh V.V., Zaitsev A.N. and Vereshchagin O.S. (2022) Nickolayite, FeMoP, a new natural molybdenum phosphide. *Mineralogical Magazine*, **86**, 749–757, https://doi.org/10.1180/mgm.2022.52.

Narayan C. and Goldstein J.I. (1985) A major revision of iron meteorite cooling rates - an experimental study of the growth of the Widmanstatten pattern. *Geochimica et Cosmochimica Acta*, **49**, 397–410, https://doi.org/10.1016/0016-7037(85)90032-8

Nehru C.E., Zucker S.M., Harlow G.E. and Prinz M. (1980) Olivines and olivine coronas in mesosiderites. *Geochimica et Cosmochimica Acta*, **44**, 1103–1118, https://doi.org/10.1016/0016-7037(80)90065-4

Pre-published article

https://doi.org/10.1180/mgm.2026.10223 Published online by Cambridge University Press

Nishinbaev T.P., Rochev A.V. and Kotlyarov V.A. (2002) Iron phosphides from combustion dumps of Chelaybinsk coal basin. *Uralian Geological Journal*, **25**, 105–114 (in Russian).

Palache C., Berman H. and Frondel C. The System of Mineralogy. 7th edition, vol. 1. New York: John Wiley & Sons, 1944, 834 p.

Pasek M.A. (2008) Rethinking early Earth phosphorus geochemistry. *Proceedings of the National Academy of Sciences*, **105**, 853–858, https://doi.org/10.1073/pnas.070820510

Pasek M. (2015) Phosphorus as a lunar volatile. *Icarus*, **255**, 18–23, https://doi.org/10.1016/j.icarus.2014.07.031

Pasek M.A. (2017) Schreibersite on the early Earth: scenarios for prebiotic phosphorylation. *Geoscience Frontiers*, **8**, 329–335, https://doi.org/10.1016/j.gsf.2016.06.008

Pasek M.A. (2019) Phosphorus volatility in the early solar nebula. *Icarus*, **317**, 59–65, https://doi.org/10.1016/j.icarus.2018.07.011

Pasek M. and Block K. (2009) Lightning-induced reduction of phosphorus oxidation state. *Nature Geoscience*, **2**, 553–556, https://doi.org/10.1038/ngeo580

Pasek M.A., Dworkin J.P. and Lauretta D.S. (2007) A radical pathway for organic phosphorylation during schreibersite corrosion with implications for the origin of life. *Geochimica et Cosmochimica Acta*, **71**, 1721–1736, https://doi.org/10.1016/j.gca.2006.12.018

Pasek M.A., Gull M., Herschy B. (2017) Phosphorylation on the early earth. *Chemical Geology*, **475**, 149–170, https://doi.org/10.1016/j.chemgeo.2017.11.008

Pasek M.A., Harnmeijer J.P., Buick R., Gull M. and Atlas Z. (2013) Evidence for reactive reduced phosphorus species in the early Archean ocean. *Proceedings of the National Academy of Sciences*, **110**, 10089–10094, https://doi.org/10.1073/pnas.1303904110

Pasek M.A. and Lauretta D.S. (2005) Aqueous corrosion of phosphide minerals from iron meteorites: a highly reactive source of prebiotic phosphorus on the surface of the early Earth. *Astrobiology*, **5**, 515–535, https://doi.org/10.1089/ast.2005.5.515

Pauly H. (1969) White cast iron with cohenite, schreibersite, and sulphides from Tertiary basalts on Disko, Greenland. Bulletin of the Geological Society of Denmark, **19**, 8–26.

Pedersen A.K. (1981) Armalcolite-bearing Fe-Ti oxide assemblages in graphite-equilibrated salic volcanic rocks with native iron from Disko, central West Greenland. *Contributions to Mineralogy and Petrology*, **77**, 307–324, https://doi.org/10.1007/BF00371560

Plyashkevich A.A., Minyuk P.S., Subbotnikova T.V. and Alshevsky A.V. (2016) Newly formed minerals of the Fe-P-S system in Kolymsky fulgurite. *Doklady Earth Sciences*, **467**, 380–383, https://doi.org/10.1134/S1028334X16040139.

Powell B.N. (1969) Petrology and chemistry of mesosiderites-I. Textures and composition of nickel-iron. *Geochimica et Cosmochimica Acta*, **33**, 789–810, https://doi.org/10.1016/0016-7037(69)90027-1

Powell B.N. (1971) Petrology and chemistry of mesosiderites-II. Silicate textures and compositions and metal-silicate relationships. *Geochimica et Cosmochimica Acta*, **35**, 5–34, https://doi.org/10.1016/0016-7037(71)90101-3

Prepublished article

https://doi.org/10.1180/mgm.2026.10223 Published online by Cambridge University Press

Pratesi G., Bindi L. and Moggi-Cecchi V. (2006) Icosahedral coordination of phosphorus in the crystal structure of melliniite, a new phosphide mineral from the Northwest Africa 1054 acapulcoite. *American Mineralogist*, **91**, 451–454, https://doi.org/10.2138/am.2006.2095

Quitté G., Birck J.-L. and Allégre C.J. (2005) Stony-iron meteorites: history of the metal phase according to tungsten isotopes. *Geochimica et Cosmochimica Acta*, **69**, 1321–1332, https://doi.org/10.1016/j.gca.2004.07.035

Rasmussen K.L., Malvin D.J., Buchwald V.F. and Wasson J.T. (1984) Compositional trends and cooling rates of group IVAB iron meteorites. *Geochimica et Cosmochimica Acta*, **48**, 805−813, https://doi.org/10.1016/0016-7037(84)90102-9

Reed S.J.B. (1965) Electron probe Microanalysis of Schreibersite and Rhabdite in iron meteorites. *Geochimica et Cosmochimica Acta*, **29**, 513−534, https://doi.org/10.1016/0016-7037(65)90044-X

Reed S.J.B. (1972) The Oktibbeha County iron meteorite. *Mineralogical Magazine*, **38**, 623−626, https://doi.org/10.1180/minmag.1972.038.297.12

Reuter K.B., Williams D.B. and Goldstein J.I. (1988) Low temperature phase transformations in the metallic phases of iron and stony-iron meteorites. *Geochimica et Cosmochimica Acta*, **52**, 617−626, https://doi.org/10.1016/0016-7037(88)90323-7

Romig A.G. and Goldstein J.I. (1981) Low temperature phase equilibria in the Fe-Ni and Fe-Ni-P systems: application to the thermal history of metallic phases in meteorites. *Geochimica et Cosmochimica Acta*, **45**, 1187–1197, https://doi.org/10.1016/0016-7037(81)90142-3

Romig A.D. and Goldstein J.I. (1980) Determination of the Fe-Ni and Fe-Ni-P phase diagram at low temperatures (700 to 300 °C). *Metallurgical Transactions*, **11A**, 1151–1159, https://doi.org/10.1007/BF02668139

Rubin A.E. and Mittlefehldt D.W. (1992) Classification of mafic clasts from mesosiderites: implications for endogenous igneous processes. *Geochimica et Cosmochimica Acta*, **56**, 827–840, https://doi.org/10.1016/0016-7037(92)90101-N

Rundqvist S., Hassler E. and Lundvik L. (1962) Refinement of the Ni_3P structure. *Acta Chemica Scandinavica*, **16**, 242–243, https://doi.org/10.3891/acta.chem.scand.16-0242

Savina E.A., Peretyazhko I.S., Khromova E.A. and Glushkova V.E. (2020) Melted rocks (clinkers and paralavas) of Khamaryn-Khural-Khiid combustion metamorphic complex in Eastern Mongolia: Mineralogy, geochemistry and genesis. *Petrology*, **28**, 431–457, https://doi.org/10.1134/S0869591120050057

Schmetterer C., Vizdal J. and Ipser H. (2009) A new investigation of the system Ni–P. *Intermetallics*, **17**, 826–834, https://doi.org/10.1016/j.intermet.2009.03.011

Scott E.R.D. (1977) Formation of olivine-metal textures in pallasite meteorites. *Geochimica et Cosmochimica Acta*, **41**, 693–710, https://doi.org/10.1016/0016-7037(77)90043-6

Sheldrick G.M. (2015) Crystal structure refinement with SHELXL. *Acta Crystallographica*, **C71**, 3–8, https://doi.org/10.1107/S2053229614024218

Schmieder M., Chennaoui A.H., Buchner E., and Tohver E. (2015) Meteorite Traces on a Shatter Cone Surface from the Agoudal Impact Site, Morocco. *Geological Magazine*, **152**, 751–757. https://doi.org/10.1017/S0016756815000047.

Pre-published article

https://doi.org/10.1180/mgm.2026.10223 Published online by Cambridge University Press

Skála R. and Cisařová S. (2005) Crystal structure of meteoritic schreibersites: determination of absolute structure. *Physics and Chemistry of Minerals*, **31**, 721–732, https://doi.org/10.1007/s00269-004-0435-6

Skála R. and Drábek M. (1999) Fe/Ni-distribution over crystallographically non-equivalent sites in the crystal structure of two synthetic schreibersites. *Lunar Planetary Science*, **30**, abstract 1553.

Skála R. and Drábek M. (2000) Variation of unit-cell dimensions of experimentally synthesized members of Fe_3P-Ni_3P solid solution. *Lunar Planetary Science*, **31**, abstract 1564.

Skála R. and Drabek M. (2003) Nickelphosphide from the Vicenice octahedrite: Rietveld crystal structure refinement of synthetic analogue. Mineralogical Magazine, 67, 783–792, https://doi.org/10.1180/0026461036740134

Stephant A., Carli C., Anand M., Neri A., Davidson J., Pratesi G., Cuppone T., Greenwood R.C. and Franchi I.A. (2022) Tissemouminites: A New Group of Primitive Achondrites Spanning the Transition between Acapulcoites and Winonaites. *Meteoritics & Planetary Science*, **58**, 111–134, https://doi.org/10.1111/maps.13944

Sugiura K., Haba M.K. and Genda H. (2022) Giant impact onto a Vesta-like asteroid and formation of mesosiderites through mixing of metallic core and surface crust. *Icarus*, **379**, 114949, https://doi.org/10.1016/j.icarus.2022.114949

Teplyakova S.N., Lorenz C.A., Ivanova M.A., Humayun M., Kononkova N.N., Borisovsky S.E., Korochantsev A.V., Franchi I.A. and Zinovieva N.G. (2022) Karavannoe: mineralogy, trace element geochemistry, and origin of Eagle Station group pallasites. *Meteoritics & Planetary Science*, **57**, 1158–1173, https://doi.org/10.1111/maps.13814

Vereshchagin O.S., Khmelnitskaya M.O., Kamaeva L.V., Vlasenko N.S., Pankin D.V., Bocharov V.N. and Britvin S.N. (2024a) Telluric iron assemblages as a source of prebiotic phosphorus on the early Earth: Insights from Disko Island, Greenland. Geoscience Frontiers, 15, 101870, https://doi.org/10.1016/j.gsf.2024.101870

Vereshchagin O.S., Khmelnitskaya M.O., Murashko M.N., Vapnik Y., Zaitsev A.N., Vlasenko N.S., Shilovskikh V.V. and Britvin S.N. (2024b) Reduced mineral assemblages of superficial origin in west-central Jordan. Mineralogy and Petrology, 118, 305–319, https://doi.org/10.1007/s00710-024-00851-8.

Vereshchagin, O.S., Gorelova L.A., Shilovskikh V.V., Vlasenko N.S., Pagano R. and Britvin S.N. (2026) Haxonite revisited, $NiFe_{22}C_6$: new crystal-chemical formulae and Fe-Ni ordering as a structure-stabilizing factor. *American Mineralogist*, **2026**, https://doi.org/10.2138/am-2025-10067, https://doi.org/10.2138/am-2025-10067

Warr, L.N. (2021) IMA–CNMNC approved mineral symbols. *Mineralogical Magazine*, **85**, 291–320, https://doi.org/10.1180/mgm.2021.43.

Wasson J.T. (2011) Relationship between iron–meteorite composition and size: compositional distribution of irons from North Africa. *Geochimica et Cosmochimica Acta*, **75**, 1757–1772, https://doi.org/10.1016/j.gca.2010.12.017

Wood, J.A. (1964) The cooling rates and parent planets of several iron meteorites. *Icarus*, **3**, 429−459, https://doi.org/10.1016/0019-1035(64)90004-1

Preprinted article

https://doi.org/10.1180/mgm.2026.10223 Published online by Cambridge University Press

Yang J., Goldstein J.I. and Scott E.R.D. (2010) Main-group pallasites: thermal history, relationship to IIIAB irons, and origin. *Geochimica et Cosmochimica Acta*, **74**, 4471–4492, https://doi.org/10.1016/j.gca.2010.04.016

Yang C.-W., Williams D.B. and Goldstein J.I. (1996) A revision of Fe-Ni phase diagram at low temperatures (<400 °C). *Journal of Phase Equilibria*, **17**, 522–531, https://doi.org/10.1007/BF02665999

Zeng X., Shang Y., Li S., Li X., Wang S. and Li Y. (2019) The layered structure model for winonaite parent asteroid implicated by textural and mineralogical diversity. *Earth, Planets and Space*, **71**, 1–15, https://doi.org/10.1186/s40623-019-1015-9

Table 1. Chemical composition of nickelphosphide (wt.%) included into this study, arranged by Ni content (ascending)

Meteorite [a]	**Classification**	**Ni**	**Fe**	**Co**	**P**	**Total**
NWA 1054[2] (a) [b]	Tissemouminite [c]	44.09	40.51	0.23	15.25	100.08
Barbianello (b)	Iron UNGR (ataxite)	46.15	38.52	0.33	15.53	100.53
NWA 1054[1] (a) [b]	Tissemouminite [c]	46.47	38.52	0.18	15.06	100.23
Brahin (d)	Pallasite PMG	47.45	37.23	0.18	15.52	100.38
Eagle Station (b)	Pallasite PES	47.95	36.54	0.26	15.24	99.99
Dorofeevka (b)	Iron IIF (Opl)	48.81	36.46	0.27	15.13	100.67
Butler (b)	Iron UNGR (Opl)	49.26	36.06	0.24	15.04	100.60
Budulan (d)	Mesosiderite B4	49.90	34.67	0.17	15.05	99.79
Mincy (d)	Mesosiderite B4	50.69	34.40	0.13	15.26	100.48
NWA 725 (c)	Tissemouminite [c]	50.31	33.57	0.27	15.31	99.46
NWA 1054[3] (a) [b]	Tissemouminite [c]	50.69	34.11	0.14	15.03	99.97
Finmarken (d)	Pallasite PMG	51.28	33.40	0.15	14.96	99.79
Hainholz (b)	Mesosiderite A4	53.71	30.85	0.15	15.01	99.72

[a] Meteorite sample sources are given in parentheses: (a) Matteo Chinellato, www.mcomemeteorite.it; (b) Renato Pagano, private donation; (c) Bruno Fectay and Carine Bidaut, www.meteorite.fr.; (d) Sergey Britvin. [b] In NWA 1054, three different nickelphosphide crystals were studied, indicated by the additional numbers in brackets. [c] Tissemouminites – a recently established meteorite group (Stephant *et al*., 2022).

Prepublished article

https://doi.org/10.1180/mgm.2026.10223 Published online by Cambridge University Press

Table 2. X-ray data collection and structure refinement summary for nickelphosphide crystals.

Crystal	Number of reflections			avg(*I*)	R_{int}	R_1	wR_2	GoF	Δρ (e Å^{-3})	
	meas.	indep.	*I*>2σ(*I*)	[σ(*I*)]					min	max
NWA 1054/2	6374	624	623	83	0.028	0.007	0.018	1.12	–0.31	0.26
Barbianello	1997	709	693	40	0.021	0.014	0.028	1.00	–0.47	0.52
NWA 1054/1	1921	624	621	39	0.036	0.012	0.029	1.03	–0.50	0.55
Brahin	4069	624	622	57	0.033	0.009	0.021	1.11	–0.34	0.33
Eagle Station	3783	624	621	38	0.045	0.011	0.027	0.93	–0.38	0.54
Dorofeevka	5142	688	687	82	0.022	0.007	0.015	1.07	–0.22	0.22
Butler	4487	562	558	51	0.037	0.011	0.024	1.10	–0.37	0.37
Budulan	5450	621	621	50	0.044	0.013	0.032	1.16	–0.59	0.53
Mincy	3617	686	685	59	0.025	0.009	0.021	1.13	–0.37	0.43
NWA 725	3194	624	622	72	0.018	0.008	0.017	1.07	–0.25	0.30
NWA 1054/3	3853	583	577	57	0.028	0.010	0.020	1.10	–0.43	0.37
Finmarken	6922	687	687	108	0.025	0.007	0.015	1.15	–0.38	0.33
Hainholz	3353	606	603	47	0.036	0.014	0.030	1.12	–0.49	0.79

Prepublished article

https://doi.org/10.1180/mgm.2026.10223 Published online by Cambridge University Press

Table 3. Refined site occupancy factors for Ni and unit-cell parameters of nickelphosphide.

Crystal	Total Ni (*apfu*) [a]		Ni, site occupancy factors			Unit-cell parameters [d]		
	EMPA [b]	Struct [c]	*M*1	*M*2	*M*3	*a* (Å)	*c* (Å)	*V* (Å^3)
NWA 1054/2	1.52	1.48	0	0.58(2)	0.90(2)	9.0183	4.4646	363.10
Barbianello	1.59	1.76	0.30(4)	0.62(4)	0.84(4)	9.0185	4.4487	361.83
NWA 1054/1	1.61	1.63	0	0.63(2)	1	9.0180	4.4625	362.91
Brahin	1.63	1.57	0	0.66(2)	0.91(2)	9.0144	4.4650	362.82
Eagle Station	1.66	1.67	0.11(3)	0.65(4)	0.91(3)	9.0188	4.4607	362.83
Dorofeevka	1.68	1.62	0.27(2)	0.55(2)	0.80(2)	9.0243	4.4501	362.41
Butler	1.70	1.74	0.27(4)	0.61(2)	0.86(3)	9.0238	4.4521	362.53
Budulan	1.74	1.72	0	0.72(3)	1	9.0100	4.4603	362.09
Mincy	1.75	1.94	0.18(2)	0.76(2)	1	9.0130	4.4585	362.18
NWA 725	1.75	1.89	0.11(2)	0.78(2)	1	9.0111	4.4615	362.27
NWA 1054/3	1.76	1.87	0.11(2)	0.76(2)	1	9.0095	4.4682	362.69
Finmarken	1.79	1.94	0.18(1)	0.76(2)	1	9.0152	4.4575	362.28
Hainholz	1.87	1.89	0.08(3)	0.81(4)	1	9.0082	4.4653	362.35

[a] Ni atoms per M_3P formula unit. [b] Electron microprobe data, estimated standard deviation 0.03 Ni *apfu*. [c] Sums of the site occupancy factors determined by the crystal structure refinements. [d]Estimated standard deviations (Rietveld refinement): 5×10^{-4} Å for the *a*-parameter, 3×10^{-4} Å for the *c*-parameter, 5×10^{-2} Å^3 for the unit-cell volume.

Prepublished article

https://doi.org/10.1180/mgm.2026.10223 Published online by Cambridge University Press

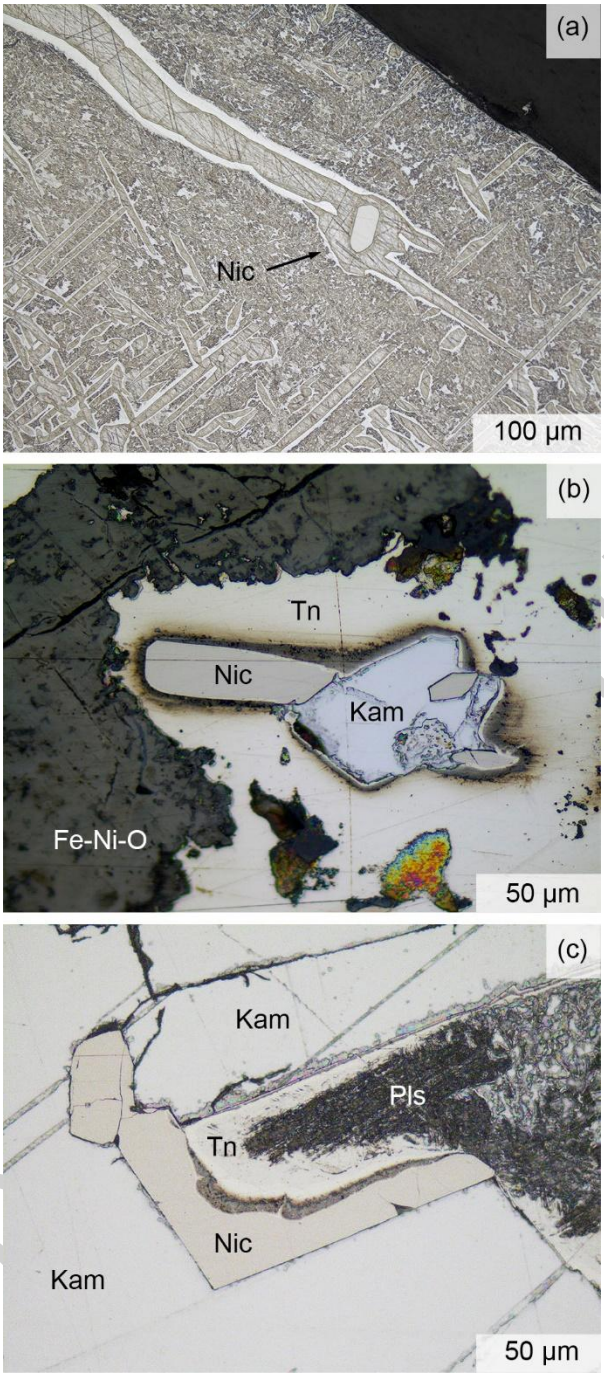


Figure 1. Nickelphosphide in studied iron meteorites and pallasites. (a) Butler; (b) Barbianello; (c) Brahin. Photomicrographs in reflected light. Abbreviations: Nic – nickelphosphide; Kam – α-(Fe,Ni) (kamacite); Tn – γ-(Fe,Ni) (taenite); Pls – plessite (micro-Widmanstätten intergrowths of α- and γ-(Fe,Ni); Fe-Ni-O – secondary Fe-Ni oxides and hydroxides. Abbreviations according to Warr (2021).

Pre Article

https://doi.org/10.1180/mgm.2026.10223 Published online by Cambridge University Press

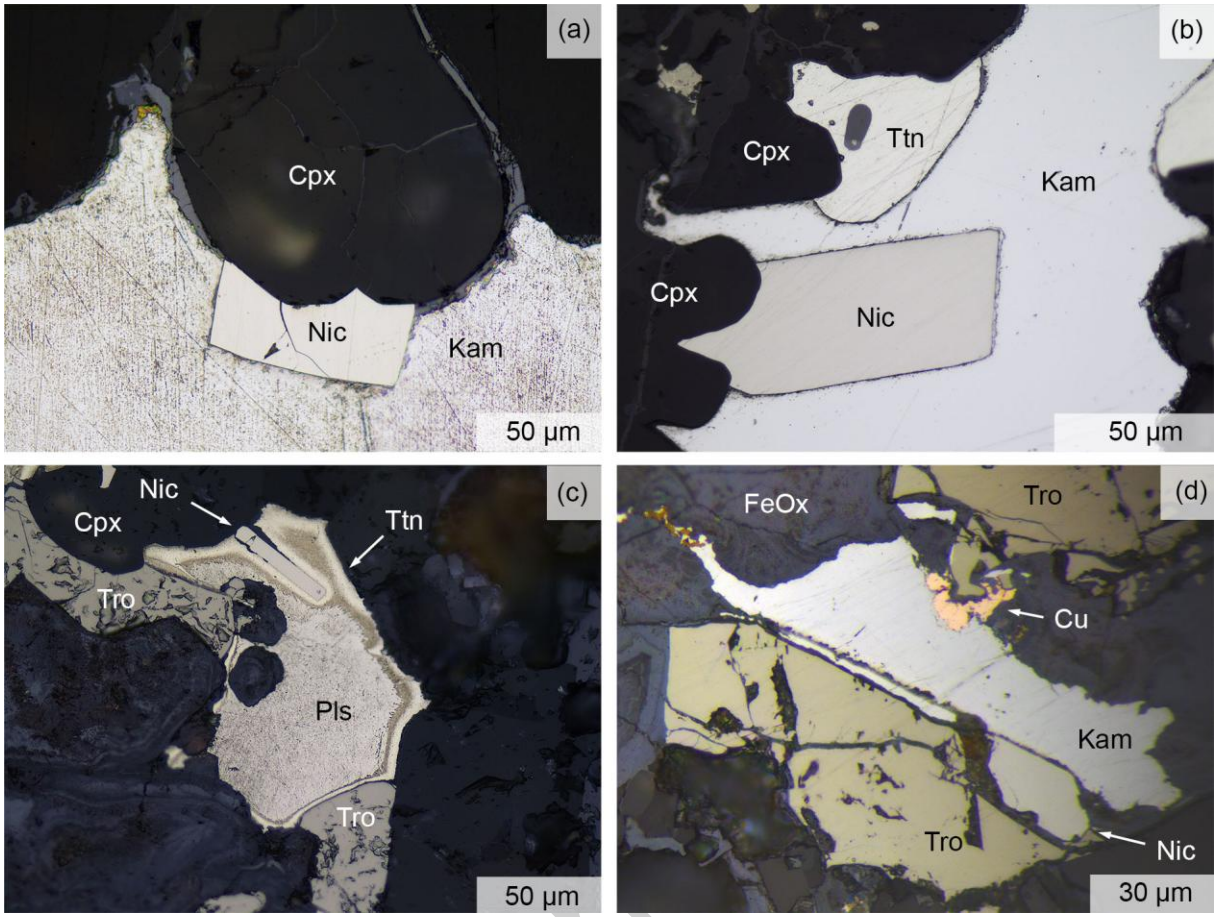


Figure 2. Nickelphosphide in mesosiderites (a,b) and tissemouminites (c,d). (a) Budulan; (b) Mincy; (c) Northwest Africa 725; (d) Northwest Africa 1054. Photomicrographs in reflected light. Abbreviations: Nic – nickelphosphide; Kam – α-(Fe,Ni) (kamacite); Ttn – tetrataenite (an ordered 50/50 FeNi); Pls – plessite (micro-Widmanstätten intergrowths of α- and γ-(Fe,Ni); Tro – troilite; Pl – plagioclase; Cpx – clinopyroxene; FeOx – secondary Fe oxides; Cu – native copper. Abbreviations according to Warr (2021).

Prepublish

https://doi.org/10.1180/mgm.2026.10223 Published online by Cambridge University Press